



WPI

Stability of ZSM-5 in Hot Liquid Water

A Major Qualifying Project

Submitted to the Faculty of

Worcester Polytechnic Institute

in partial fulfillment of the requirements for the

Degree in Bachelor of Science

in

Chemical Engineering

By

Ibrahim Abu Muti

Abdullah Almaymuni

Nyoca Davis

Iordanis Kesisoglou

Date: 04/28/16

Project Advisors:

Michael T. Timko, Advisor

Nathaniel A. Deskins, Co-Advisor

This report represents work of WPI undergraduate students submitted to the faculty as evidence of a degree requirement. WPI routinely publishes these reports on its web site without editorial or peer review. For more information about the projects program at WPI, see <http://www.wpi.edu/Academics/Projects>.

Abstract

Zeolites are a class of microporous crystalline aluminosilicate catalysts. The catalytic activity is determined by the aluminum content in the framework. Zeolite Socony Mobil-5 (ZSM-5) has an inverted mordenite framework (MFI) structure. ZSM-5 is commonly utilized in gaseous phase reactions. Recent interest for oil upgrading and new technologies in biofuel production suggest that ZSM-5 has advantages in aqueous phase reactions. The challenge is that the catalytic activity of ZSM-5 is greatly impacted by framework decrystallization in hot liquid water (HLW). In this study, we investigated the rate of ZSM-5 framework decrystallization in HLW at temperatures ranging from 150 °C to 350 °C and times ranging from 6 hours to 1000 hours. The changes in crystallinity of the treated ZSM-5 samples were analyzed over time using x-ray diffraction. Tracking ZSM-5 crystallinity over time indicates that decrystallization in HLW obeys a pseudo-first order rate law. Temperature analysis of the pseudo-first order rate constant indicates that ZSM-5 decrystallization in HLW follows a non-Arrhenius behavior due to the dissociation of zeolite acid sites in water. Supporting data from IR and gas sorption indicates that the decrystallization mechanism of ZSM-5 in HLW is dealumination. The decrystallization of ZSM-5 in HLW appears to take place due to thermal and ionic effects. The thermal effect originates from high temperatures and the ionic effect is due to a combination of auto-ionization of water and the ZSM-5 acidity.

Acknowledgements

The WPI Zeolite Hydrothermal Stability MQP team would like to extend our appreciation to the following individuals for their guidance and support of this project:

- Professor Timko, Professor Deskins, Professor Sisson, Professor Tompsett, and Thomas Partington
- Timko's Lab: Alex Maag, Avery Brown, Maksim Tyufekchiev, and Azadeh Zaker.
- Sisson's Lab: Yang Zi
- WPI Chemical Engineering Department
- Saudi Aramco provided partial funding for this work.

Table of Contents

Abstract	2
Acknowledgements	3
List of Figures	5
1. Introduction	6
2. Background	8
2.1 Zeolite.....	8
2.2 ZSM-5	8
2.3 Hydrothermal Water	10
3. Methodology	12
3.1 Reactor Preparation	12
3.2 Catalyst Preparation	13
3.3 Experiment	13
3.4 Analytical tools.....	13
3.4.1 Scanning Electron Microscope.....	13
3.4.2 X-Ray Diffraction.....	14
3.4.3 Gas Sorption	15
3.4.4 Infrared DRIFTS	16
4. Results	18
4.1 Scanning Electron Microscopic (SEM).....	18
4.2 X-Ray Diffraction (XRD)	19
4.3 Gas Sorption	22
4.4 Infrared Red (IR)	24
5. Discussion	26
5.1 Non-Arrhenius Decrystallization Behavior.....	26
5.3 Decrystallization Mechanism	31
6. Conclusion.....	33
7. Recommendations	34
8. References	39
Appendix	42
Tables of relative crystallinity results	42
MQP Poster	43

List of Figures

Figure 1: showing the pentasil structure and Cage structure of ZSM-5 modeled by IZA-SC	9
Figure 2: showing pore channel in ZSM-5.....	10
Figure 3: water properties versus temperature change	11
Figure 4: Setup and schematic drawing of the apparatus	12
Figure 5: X-Ray Diffraction Wide Scan Pattern of Zeolite ZSM-5 ratio 20 ASTM reference	15
Figure 6: The IR result obtained of an untreated calcined sample	17
Figure 7: showing isotherms of dealuminated and desilicated H-ZSM-5.....	18
Figure 8: showing SEM images of ZSM-5 after treatment	19
Figure 9: showing diffraction peaks for treated ZSM-5 samples	20
Figure 10: showing diffraction peaks for treated ZSM-5 samples	22
Figure 11: Infrared Red results at 150 °C	24
Figure 12: Infrared Red results at 250 °C and 350 °C	25
Figure 13: Isotherms of treated samples at different temperature for 18hs (300 and 350 °C) 12hrs (250 °C) ..	26
Figure 14: Relationship between Surface Area and % Crystallinity	27
Figure 15: Measured pH level results	29
Figure 16: Natural logarithm of the real rate constant versus 1/T	30
Figure 17: Showing decrystallization mechanisms	31
Figure 18: Showing isotherms of dealuminated and desilicated H-ZSM-5	32
Figure 19: The 5T model	36
Figure 20: The 12T model	36
Figure 21: The Embedded ONIOM model	37
Figure 22: The MQP project poster	43

1. Introduction

Zeolites belong to a class of microporous crystalline aluminosilicate catalysts that are defined by their structure and composition.¹ They are very attractive catalysts that are synthesized from abundant low cost materials, have a well-defined pore structure and high activity per acid site.² Zeolites have acidic catalytic properties that arise from aluminum in the framework. An example of a high-silica zeolite is Zeolite Socony Mobil-5, ZSM-5. It is a member of the pentasil family and is represented by the formula $\text{Na}_n\text{Al}_n\text{Si}_{96-n}\text{O}_{192}\cdot\text{H}_2\text{O}$ where n is less than 27. ZSM-5 has an inverted mordenite framework (MFI) structure. The structure enhances a product's selectivity due to the steric nature of ZSM-5 with this framework consisting of a two-dimensional network of 5-6Å intersecting micro channels. The selectivity and activity of ZSM-5 enable it to be utilized in a wide range of industrial applications. These applications include petrochemical processes such as catalytic cracking, alkylation of benzene, toluene disproportionation, xylene isomerization, and methanol to gasoline process.³ ZSM-5 can be used under steaming and hot liquid water conditions.

Many studies have investigated the stability of ZSM-5 under steaming conditions due to its wide use in gas phase reaction. In the presence of steam, the framework aluminum (Al) atoms in ZSM-5 are removed from the lattice.⁴ This process is called dealumination. The Al atoms then form an independent alumina phase, called extra framework aluminum (EFAl), outside the zeolite crystal to produce isolated charge-compensating cations.⁵ The Al content controls the degree to which zeolites are dealuminated by steaming. The stability of ZSM-5 under steaming conditions decreases with increasing Al content.⁶ Previous studies noted that EFAl improves the hydrothermal stability, increases Lewis acidity, and enhances catalytic activity for reactions.^{4a, 7}

Many biofuel technologies have focused attention on the use of ZSM-5 in hot liquid water (HLW). The application of hot liquid water in chemical reactions is characterized by the wide range of conditions and the exceptional change of properties of the reaction medium.^{5b, 8} There is a possibility that decrystallization of ZSM-5 in HLW is due to thermal and hydrolysis effects. The thermal effect originates from high temperature, which increase the vibrational frequency of the molecules to the point where bond dissociation takes place. The hydrolysis effect is due to the auto-ionization of water, which produces hydronium and hydroxyl ions at high temperatures. The interaction of zeolite

and HLW is dependent on the hydrophilic or hydrophobic characters of the zeolite surface. Water can diffuse into the cavities of the zeolites. If the zeolite contains hydrophilic site, such as silanol defects (Si-OH), it can act as a nucleation site for water condensation. This defect in the zeolite increases the amount of water adsorbed on the zeolite. The hydrophobicity of ZSM-5 is controlled by the Si/Al ratio (Brønsted acid sites), the density of the silanol group, and extra framework Al ions.^{2,7,9}

The hydrolysis effect takes place by two mechanisms: acid-catalyzed (dealumination) and/or base-catalyzed (desilication). The two reaction mechanisms may occur simultaneously but it is likely that one is more dominant than the other. Many studies proposed that dealumination is the dominant degradation pathway under steaming conditions of ZSM-5.^{2,7,9} In hot liquid water, a study proposed that the stability of zeolites strongly depends on their framework type where ZSM-5 has shown stability in HLW up to 200 °C and 6 hr treatment time, while faujasite (FAU) zeolite Y degradation is dependent on its Si/Al ratio.² The study proposed that desilication is the dominant mechanism in the decrystallization of zeolite Y in HLW.² Resasco et. al. studied the factors that affect stability of ZSM-5 in HLW and showed that Brønsted acid sites, Si-O-Si bonds, framework type, silanol defects, and extra framework Al could influence the stability of zeolite in liquid water.^{1a}

Studies show that, after treatment in hot liquid water at 200 °C, the zeolite Y structure may collapse and lose its crystallinity.^{2,5} The stability of ZSM-5 has only been studied in HLW in conditions of 200 °C and 6 hrs.² These conditions are not relevant to many industrial processes. The observed decrystallization of ZSM-5 is very problematic in bio-upgrading applications such as dehydration, deoxygenation, alkylation and aldol condensation that require zeolite in hot liquid water.^{1a} For this reason, this investigation seeks to establish a fundamental understanding of the hydrothermal stability of ZSM-5 in HLW. To achieve this goal, we measured the crystallinity of ZSM-5 after treatment in HLW. Experiments were conducted for different periods of time in a batch reactor. Each treated ZSM-5 sample was analyzed using different physiochemical techniques. The techniques include Scanning Electron Microscopy (SEM), X-ray Diffraction (XRD), Infrared Spectroscopy (IR), and gas sorption. The changes observed using these tests were used to understand the stability of ZSM-5 in HLW. Crystallinity data were analyzed to determine the rate of decrystallization of ZSM-5, and hence shed light on the mechanism of ZSM-5 decrystallization.

2. Background

2.1 Zeolite

Zeolites are one of the most diverse and industrially useful mineral groups. They are crystalline solids structures made of silica and alumina that form a framework with an open three-dimensional tetrahedral structure. Silicon can be substituted with aluminum, which creates a charge imbalance and requires other cations to be present in order to balance the charge distribution. Zeolites can be classified by both the ratio of silica to alumina and the framework type.

Zeolites can sometimes be referred to as molecular sieves since zeolites can separate molecules based on differences in size, shape, and polarity. This property originates from the porosity of zeolite. The small pores in zeolite only allow certain size of molecules to be adsorbed. The charge-balancing cations can affect the size of the pore; for example, the sodium form of Zeolite A has a pore size of approximately 4 Å. If Na^+ is exchanged with the larger K^+ , the pore opening is reduced to 3 Å.¹⁰ The selectivity of zeolite depends on the shape of the molecule. Furthermore, the zeolite selectivity depends on the polarity of the molecule, so high silica zeolites are organophilic whereas low silica zeolites are hydrophilic.

Zeolites are capable of acting as catalysts in chemical reaction. The large surface area that zeolites have make them prominent in heterogeneous reactions. In fact, zeolites are cost efficient, as they can be reused after the reaction as the case with zeolite ZSM-5 in the catalytic cracking of crude oil. Furthermore, the ability of exchanging cations in the zeolite framework provides a wide range of zeolite uses as a reaction catalyst. The pore channels structure of zeolite enhances the catalyst selectivity by first allowing only the molecules that have size similar to the pores to diffuse, second zeolites limit the reaction product that form by going through large transition state configuration.

2.2 ZSM-5

One of the most important and widely used zeolites is Zeolite Socony Mobile-5 (ZSM-5). It was first synthesized by Mobile Oil Company in 1975. ZSM-5 is a high silica zeolite that belongs to the pentasil family. A pentasil unit is composed of eight five-membered rings as shown in Figure 1a. The vertices in each ring are either aluminum or silicon, and oxygen is bonded between the vertices. There

are two types of pore channels in ZSM-5, both of which are composed of a ten-membered ring; when the straight and sinusoidal channel intersects, a cage is formed, shown in Figure 1b. The pore diameter in ZSM-5 is around 5.5 Å, each cage has a diameter of around 7 Å as shown in Figure 2. The ZSM-5 crystallographic unit cell contains 288 atoms, 81 channels, and 12 cages. The total pore volume of ZSM-5 is 0.242 cm³/g that is 45% of the zeolite's total bulk volume.¹¹

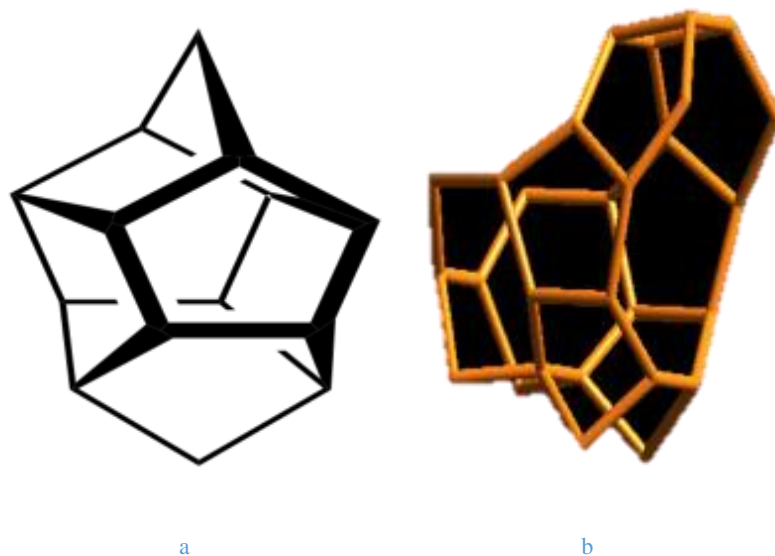


Figure 1: showing the pentasil structure (left) and Cage structure of ZSM-5 modeled by IZA-SC (right) ¹¹

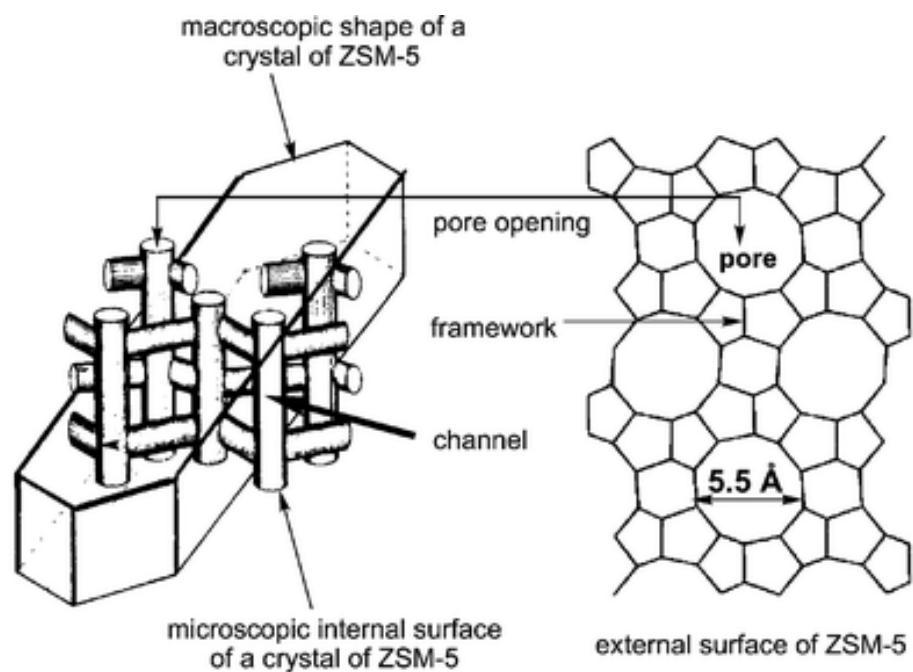


Figure 2: showing pore channel in ZSM-5 ¹²

2.3 Hydrothermal Water

Hydrothermal water (HTW) is water that is either at hot liquid water conditions of temperatures above 100 °C, or supercritical conditions at temperatures higher than 374 °C and pressure higher than 218 atm. HTW has unique properties where they have been studied with a variety of experimental and computational techniques in order to provide important clues for understanding the solvent effects on chemical reactions under these conditions. Hydrogen bonding is the source of many of the unique properties of liquid water where they become weaker with increasing temperature and decreasing density.¹³ The structural changes of hydrothermal water affect the dynamics of its molecules. Water polarity decreases in the comparison from ambient to supercritical conditions. That is because physicochemical properties such as the dielectric constant decreases at ambient conditions to a value common to normal solvents at supercritical conditions indicating changing in its organophilicity at supercritical conditions.² Water autoionization which gives rise to its pH is an important key to study water properties. At ambient conditions in water molecules, one in $\sim 6 \times 10^8$ molecules are auto ionized as it yields the natural value, due to K_w of water is 10^{-14} and due to its natural nature, half of them are protons at ambient conditions showing $pH = (1/10^{-7}) = 7$ where

pH is the negative logarithm of proton activity.¹⁴ Previous studies showed that ionic product of water increases with increasing the temperature until the critical point where it shows quick drop.⁸ Dielectric constant is an important property that represents the solvent's ability to accept ions. According to previous studies, it decreases with increasing temperature.¹⁵

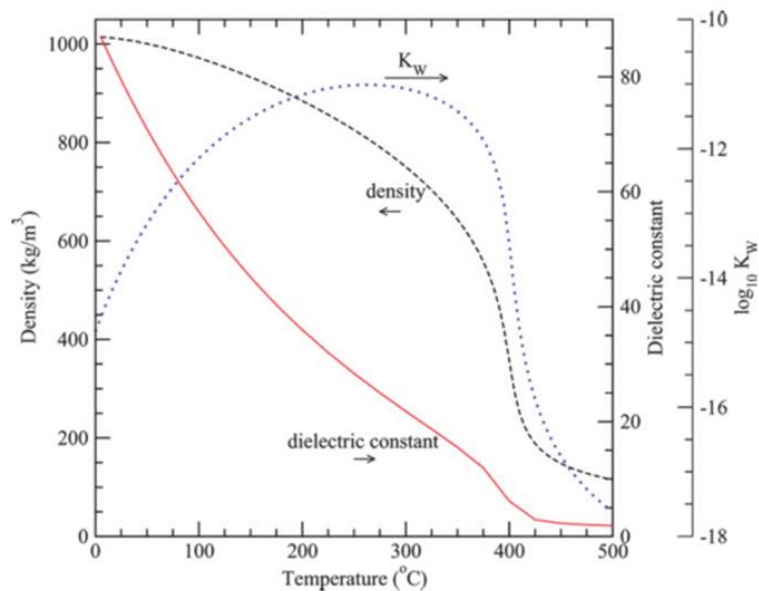


Figure 3: water properties versus temperature change¹⁵

3. Methodology

3.1 Reactor Preparation

A 100 ml Parr stirred reactor vessel, model 452HC2 made of Hastelloy, was used to perform batch experiments for this research. The reactor was loaded with distilled water at half of its volume. Nitrogen gas at 3000 psig was introduced to the system. The reactor was pressure tested and monitored for 24 hours to ensure that the reactor could withstand the pressure, followed by a similar examination at higher temperature condition.

Figure 4 contains a photograph of one of the reactors that was used in this work and a schematic of the apparatus. After pressure testing the reactor, DI water and zeolite powder were placed inside the reactor. To monitor the operating conditions of the reactor a pressure gauge and thermocouple were installed. The reactor is pressurized using a nitrogen gas tank. The thermocouple is connected to a process controller to change and monitor the temperature of the reactor. The temperature controller included a safety cutout in the case of overheating and a safety button in case of reactor leakage. The safety cutout button is set so that it pops up when the temperature increases to a higher point than the desired. When the safety button is triggered, the heating is terminated to prevent any accident. An agitator is used to keep the liquid water temperature uniform and the zeolite properly suspended in the solvent. Finally, a chiller, model 1146 by Polyscience, was used to keep the mixer ball bearings from overheating.

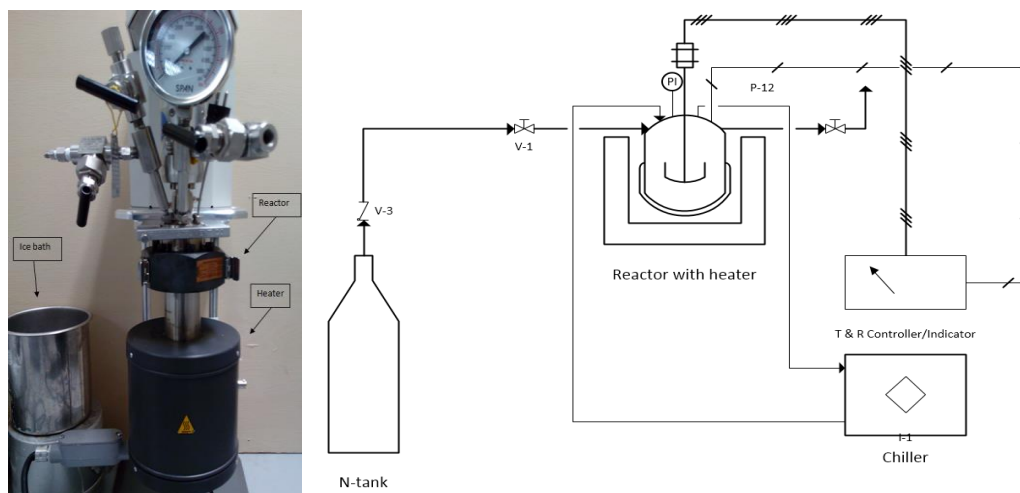


Figure 4: Setup and schematic drawing of the apparatus

3.2 Catalyst Preparation

The zeolite used in this study was ZSM-5 (Si/Al = 38) supplied by ACS Materials in the H form. Prior to each experiment, 1.3 g of the zeolite was measured and placed in an oven at 100°C for 1 hour. The sample was transferred to an oven at 550 °C, 48000 Thermolyne Furnace, to be calcined for approximately 16 hours. The first 100 °C oven of utilized to evaporate any water remnants from ZSM-5 sample. The calcination transformed the NH₄-form zeolite to H-form zeolite. Also, the second oven at 550 °C was used to pristine our sample from any organic residues due to the synthesis process of ZSM5.

3.3 Experiment

The experiment was initiated by introducing 1g of the calcined zeolite sample in the Parr reactor followed by adding 40 mL of DI water. The agitator and thermocouple were connected to the reactor. The system was pressure tested with nitrogen gas at 1000 psig for 15 minutes. The reactor was purged 5 times to remove the oxygen from the system. The reactor was initially pressurized using nitrogen gas at 1000 psig, to ensure the water remains liquid at high temperature. The reactor was heated to the desired temperature followed by adding nitrogen gas to reach the desired pressure for the run, and then the time was recorder. When the desired time was met, the heater and agitator were powered off. The reactor was cooled in an ice bath and slowly depressurized inside the fume hood. The heating and cooling time for the experiment was measured and recorded. The mixture in the reactor was removed and dried in an oven, VWR 1350F, at 60°C for 15 hours. After which the zeolite sample was analyzed.

3.4 Analytical tools

3.4.1 Scanning Electron Microscope

Scanning Electron Microscope (SEM) is a microscope that uses electrons to form an image. SEM images contains information about a sample's surface topography and composition. A beam of electron produced by an electron gun, located at the top of the microscope. The beams follow a vertical path through the microscope, then through electromagnetic fields and lenses. When the beam comes in contact with the sample, the electrons and X-rays in the sample are ejected. Detectors

collect these X-rays and backscattered electrons and secondary electrons and convert them into a signal that is then converted to an image.

A JOEL JSM-7000F SEM, located in Higgins Labs, was used to produce SEM images of seven samples of the treated ZSM-5 to compare the changes in ZSM-5 morphology when i) treated for the same time at different temperatures and ii) when treated at the same temperature for different times. Each dried treated sample was first placed on a specimen stub and then sputter coated with Palladium to ensure that the surface of the sample was electrically conductive and electrically grounded to prevent the accumulation of electrostatic charges at the surface. The coated samples were then placed in the JOEL JSM-7000F SEM to be analyzed.

3.4.2 X-Ray Diffraction

X-Ray powder Diffraction (XRD) is used in this research to analyze the relative crystallinity of ZSM-5. This analytical technique can detect changes in the crystalline structure of ZSM-5 that result from the hydrothermal treatment. XRD measures the bulk framework crystallinity. XRD is a leading indicator to the stability of ZSM-5 under hydrothermal conditions since any decrystallization to the treated ZSM-5 sample can be seen as a decrease in the relative crystallinity measured by the XRD.

XRD instrument is supplied by Rigaku with a model number GD2820. The XRD instrument consists of three basic elements: An X-ray tube, a sample holder, and an X-ray detector. The X-ray, in most of the XRD diffractometers, is produced by dislodging the inner shell electrons of copper with accelerated electrons produced by heating filament in a cathode ray tube. The X-ray is then collimated and directed onto the sample. The sample holder is rotated with an angle θ relative to the X-ray, the reflected X-ray is recorded by the sample detector which rotates with twice the angle 2θ as sample holder.

The XRD results are presented as graph that has the intensity in the y-axis and the (2θ) in the x-axis. The graph shows the peak intensity that corresponds to a specific angle of detection as shown in Figure 5. The peaks are results of the diffracted X-ray by the crystalline lattice of the sample that show the XRD pattern of the sample. XRD diffraction was performed in the range of 5-80 (degree) with a step size of 0.5 and a 1 second dwell time. According to the American Society for Testing and Materials (ASTM, D5758) there are two methods for calculating the relative crystallinity: Integrated

Peak Area Method and Peak Height Method.¹⁶ The integrated peak area method is the most common method; therefore, it was used also in this research. The integrated peak area method calculates the sum of the area under the peaks that corresponds to the angles between 22.5° to 25.0°. The calculated area of the hydrothermally treated ZSM-5 sample was divided by the calculated area of the calcined ZSM-5 sample to calculate the relative crystallinity of treated ZSM-5 sample.

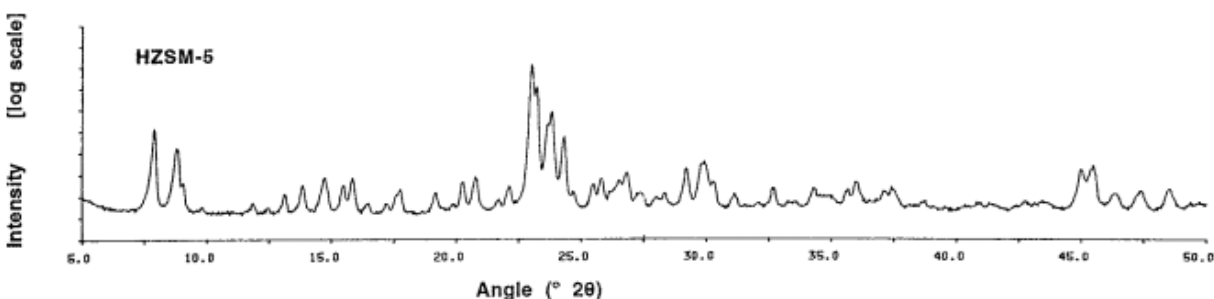


Figure 5: X-Ray Diffraction Wide Scan Pattern of Zeolite ZSM-5 ratio 20 ASTM reference.

3.4.3 Gas Sorption

Gas adsorption is used to make surface area and porosity measurements for porous materials. This method involves exposing the solid materials with gases or vapors at a variety of conditions and evaluating either the weight uptake or the sample volume. Analysis of the data gives information about physical characteristics, such as skeletal density, porosity, total pore volume, and pore size distribution of the solid. The Brunauer-Emmett-Teller BET is the most common method used for the determination of surface area of powders and porous materials and the most commonly used gas is nitrogen.¹⁷

A Quantachrome Instruments Autosorb®iQ instrument was used to determine the BET area, micropore volume and area for the ZSM-5 samples in this investigation. Approximately 0.025g of a ZSM-5 sample was first degassed, to remove physisorbed molecules. The samples were outgassed at 60, 80, 100 and 120 °C. Finally the temperature was increased to 350 °C. The degassed sample was then dosed with argon from a p/p₀ range of 10⁻⁶ to 0.99. p/p₀ is known as the gas' relative pressure, where p is the partial vapor pressure of adsorbate gas in equilibrium with the surface at the boiling point of liquid nitrogen (77.4K) and p₀ is the saturated pressure of the adsorbate gas (argon). The relative pressure p/p₀ is related to the volume of the gas adsorbed at standard temperature and pressure and the BET area by the equation below:

$$\text{BET Area} = \frac{1}{V_{\text{volume}} \left(\frac{p_0}{p} - 1 \right)}$$

The sample was cooled in liquid nitrogen and maintained at -196°C for the duration of the isotherm. The Dubinin Radushkevich (DR) method was applied to the isotherms to determine surface area of each. The changes in the surface area observed in the samples overtime gave an indication in the changes in the porosity of the ZSM-5 over time.

3.4.4 Infrared DRIFTS

Fourier Transform InfraRed, FT-IR spectrometer was utilized to identify functional groups in a sample. The FT-IR spectroscopy, Nicolet Magna IR 560 instrument, was used. The IR instrument can provide information on the chemical composition of a sample.¹⁸ IR has been useful in the aspects and fields of studying zeolite chemistry. The IR spectra, as shown in Figure 6, provide information on zeolite formation, framework vibrations, surface property, adsorption and catalytic activity.

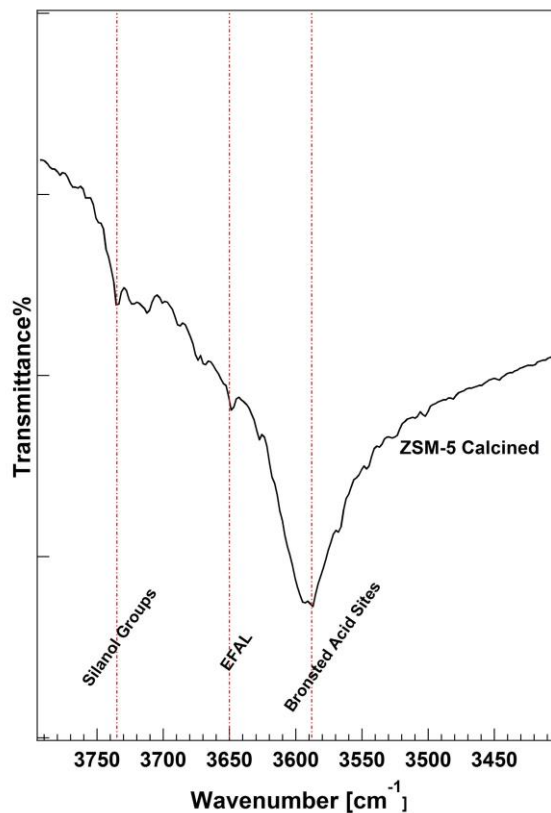


Figure 6: The IR result of untreated calcined sample

IR analysis was performed on calcined and hydrothermally treated samples. A DRIFTS cell was loaded with ZSM-5 followed by purging the system with N₂ for 10 minutes. To remove carbon dioxide, the cell temperature was increased by 20 °C increments at 20 min intervals until 120°C, where it was held for 30 minutes before raising 50°C increments to 550°C. The spectral range analyzed was from 2000-4000 cm⁻¹.¹⁹

4. Results

4.1 Scanning Electron Microscopic (SEM)

Scanning Electron Microscope was used to examine the morphology of the treated zeolite samples. SEM images, as seen in Figure 7 reveals that increase in the treatment temperature and time lead to a decrease in the well-defined crystalline structure of the zeolite, and an increase in the population density of a “flower-like” feature.

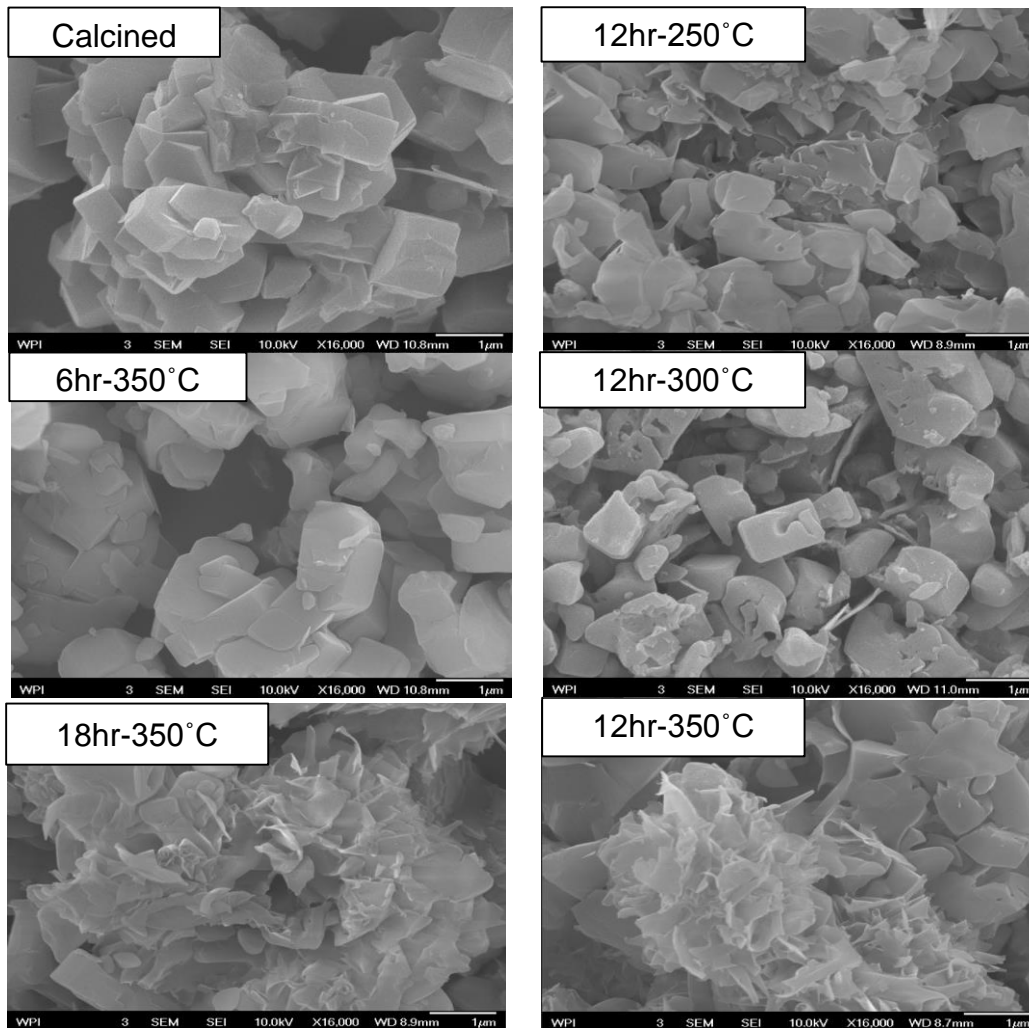


Figure 7: showing SEM images of ZSM-5 after treatment

4.2 X-Ray Diffraction (XRD)

X-Ray Diffraction instrument was used in our research in order to investigate the crystallinity of the treated zeolite sample. Figure 8 shows representation of XRD data.

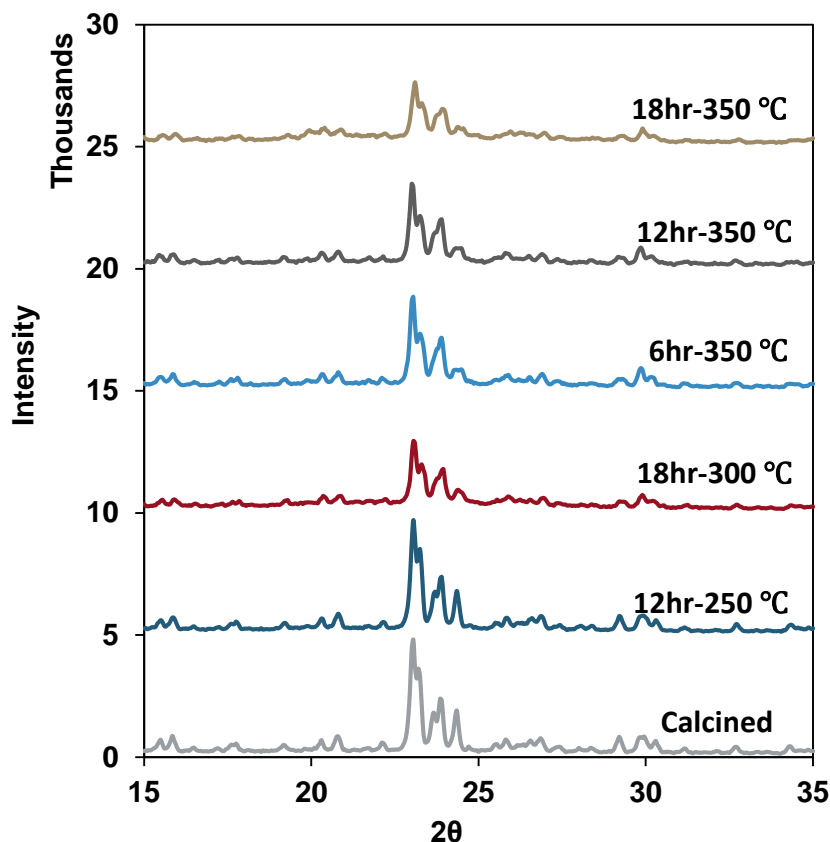


Figure 8: showing diffraction peaks for treated ZSM-5 samples

The loss in crystallinity can be seen in the graph as a decrease in the intensity of the major peaks (20° - 25°). As seen in the graph, increasing the treatment temperature decreases the peak intensity which implies a decrease in the crystallinity of the sample. Also, increasing the treatment time decreases the crystallinity of the sample. Since the XRD diffraction peaks show a loss in crystallinity, then the “flower-like” feature that was seen in the SEM pictures can signify an amorphous structure.

To quantify this XRD data, the relative crystallinity of the treated samples was calculated using the integrated peak area method as explained in the methodology. Figure 9 shows the relative crystallinity as a function of treatment time.

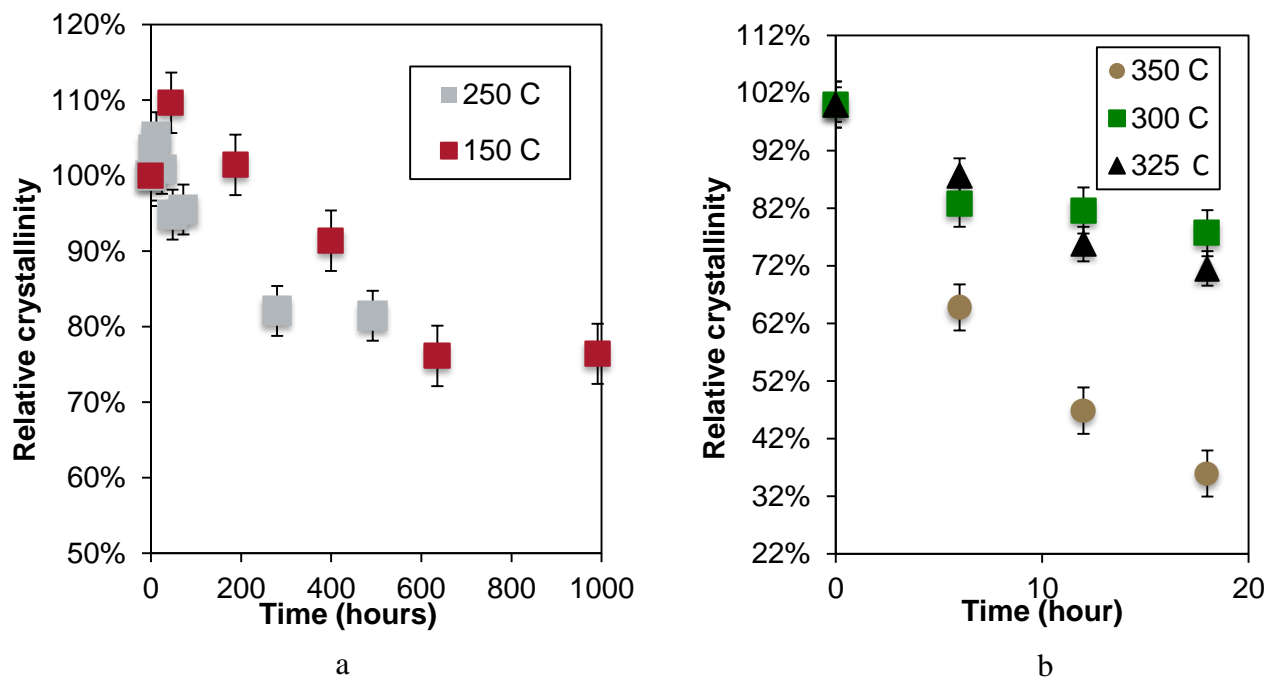


Figure 9: relative crystallinity as function of time

Figure 9a shows the relative crystallinity at temperatures 150 °C and 250 °C. At these low temperatures long-term treatment was performed over the course of hundred of hours in order to have an idea of the extent of ZSM-5 stability in HLW. Figure 9a show that after approximately 1000 hours of treatment at 150 °C, the zeolite shows a relative crystallinity of 76% \pm 4%. Also, at 250 °C the sample shows a relative crystallinity of 81% \pm 4% after a 500 hours treatment. The data points collected at both 150 °C and 250 °C follow similar trend. Initially, there is an increase in relative crystallinity due to the removal of some amorphous phase from the zeolite. Then, the decrystallization of the zeolite takes place at different rates depending on the treatment temperature; the higher the temperature the higher the decrystallization rate.

The zeolite comes to a point where it shows stability around 75% relative crystallinity. The stabilization effect is believed to be due to the effect of the extra-framework aluminum (EFAl), which is generated during the decrystallization of the sample. Studies in the literature proposed that EFAl protects the zeolite framework by blocking the silanol groups from being attacked by water molecules since silanol groups are considered to be the most susceptible place for water to attack.^{1a, 20}

Figure 9b shows the relative crystallinity at temperatures 300 °C, 325 °C, and 350 °C. The higher temperature resulted in a more rapid decrystallization rate. Moreover, the stability that was seen at lower temperature around a relative crystallinity of 75% is absent at high temperatures especially at 350 °C. That can be attributed to the idea that high temperature can overcome the energetics of EFAl protection. It can be reasoned that high temperature results in the movement of EFAl since it is hydrogen bonded with the silanol groups and the increase in temperature can decrease this bonding effect.

At high temperature 300 °C, 325 °C, and 350 °C the heating time was around 40 minutes. The research team suspected that decrystallization might take place during the heating time. Therefore, several runs were performed in order to investigate the heating and cooling effect. The relative crystallinity of the samples at high temperature after the heating and cooling experiment showed a loss of around 20% crystallinity. This was taken into account by redefining the initial crystallinity as the one measured after the heating and cooling run. The graph of high temperature was normalized on 80% relative crystallinity in order to have a more accurate measurement of the relative crystallinity as a function of time.

4.3 Gas Sorption

Nitrogen Sorption was used to study the porosity and surface area of the untreated (calcined) and treated zeolite samples. Figure 10 shows the isotherms for the calcined sample and the treatment samples 250°C at 12 hrs and 300°C and 350°C at 18hrs. The isotherms show the relationship between the relative pressure (p/p_0) and the volume of the gas adsorbed at standard temperature and pressure for the respective samples. The adsorption isotherm is achieved by measuring the amount of gas adsorbed for the range of p/p_0 at constant temperature, and the desorption isotherm is achieved by measuring the gas removed as pressure is reduced. Both the adsorption and desorption isotherms follow a similar pathway. Additionally, as the treatment temperature of the sample increased, the volume of gas adsorbed decreased.

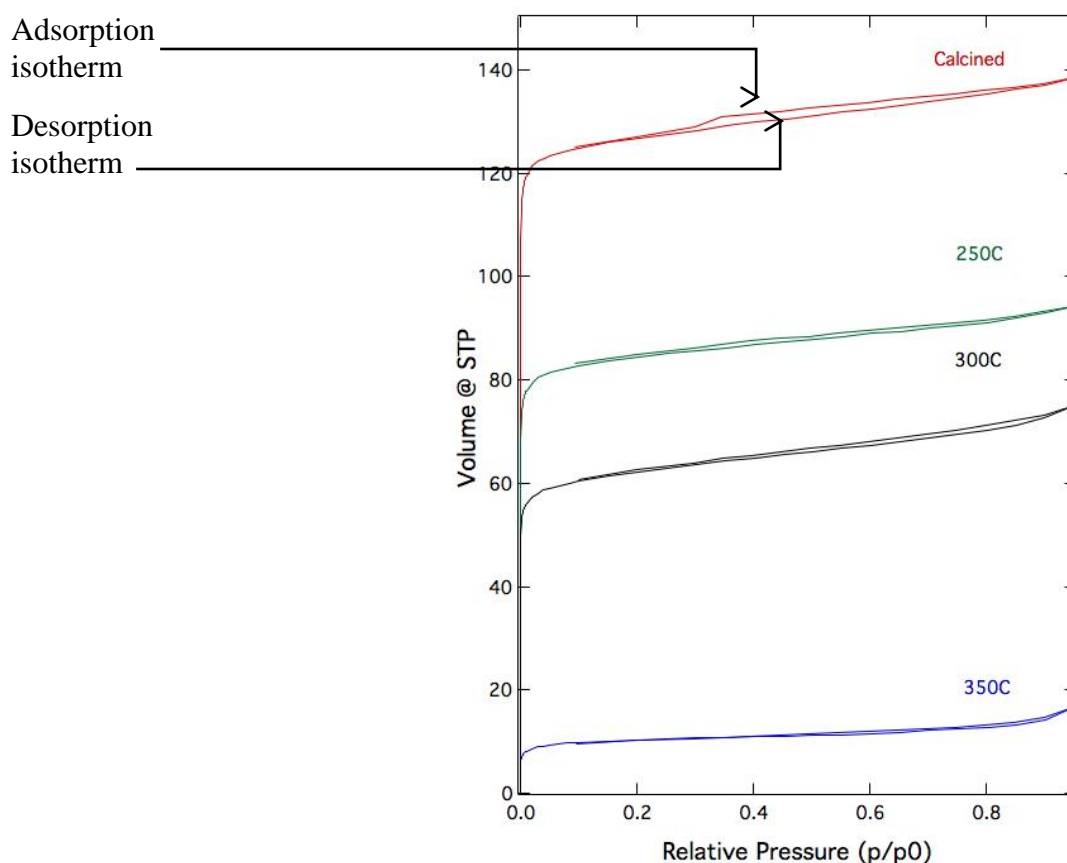


Figure 10: Isotherms of treated samples at different temperature for 18hs (300 °C and 350 °C) 12hrs (250 °C)

The total pore volume (porosity) is directly related to the volume of gas adsorbed at a relative temperature. Therefore, based on Figure 10, it can be concluded that the porosity of ZSM-5 decreases as the treatment time and temperature increases.

Using the BET feature of the Quantachrome Instruments Autosorb®iQ instrument software, the surface area associated with each treated sample was obtained. Table 1a provides BET Surface Area (in m²/g) for the samples treated at 300°C and 350°C for 6 and 18hrs and Table 1b provides BET Surface Area (in m²/g) for the samples treated at 250°C and 350°C for 12, 24 and 492 hrs. When compared with the calcined sample, the data indicates that increasing the treatment time and temperature yields a general trend of decreasing BET surface area of ZSM-5.

Table 1: Changes in surface area as functions of temperature and time

a)

Time (s)	Surface Area (m ² /g)	
	300 °C	350 °C
Calcined	419.511	419.511
6	210.55	326.862
18	195.625	32.688

b)

Time (s)	Surface Area (m ² /g)
	250 °C
Calcined	419.511
12	291.778
24	252.331
492	91.94

4.4 Infrared Red (IR)

To obtain more insight regarding the mechanisms, we turned to IR spectroscopy. IR gives more understanding by providing qualitative data to study the treatment effects on the functional groups. From the framework vibrational spectra for treated sample at 150 °C (Figure 11), structural changes during treatment can be identified. The bands around 3550-3650 cm^{-1} have been assigned to the presence of Brønsted Acid Sites (BAS). These bands are observed to decrease when compared to treated samples in HLW at 500 hours and 991 hours. The bands around 3650-3700 are assigned to the presence of extra framework aluminium which is observed to be generated at the treated sample at 991 hours.²¹ The presence of silanol groups at the bands of 3750 are observed to be decreasing relatively to the peaks of BAS and EFAL.

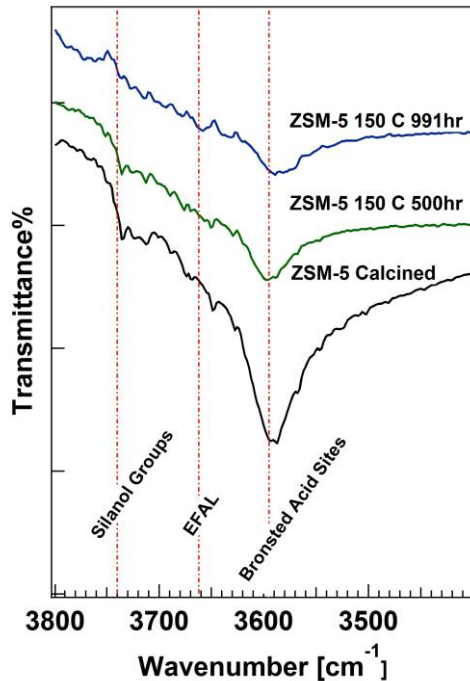


Figure 11: Infrared Red results at 150 C

In Figure 12, FTIR spectra of before and after HLW treatment are shown for samples at 250 °C and 350 °C. The rate of loss of BAS and silanol groups were observed to be higher when compared to the treated sample at 150 °C (figure 11). At 250 °C, the samples showed faster appearance of EFAL at 48 hrs, while the presence of BAS still exists after treatment for 492 hr. At 350 °C, the treated samples showed faster presence of EFAl after 6 hrs of treatment while the DRAFT results showed higher generation of EFAl relativity to BAS presence.

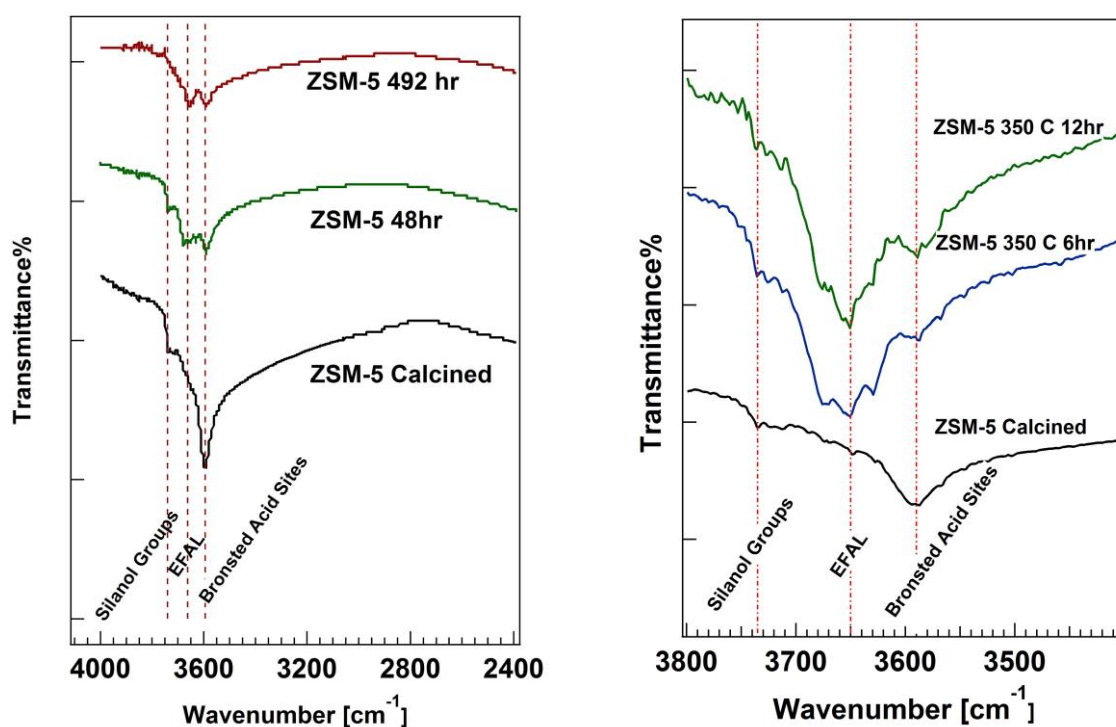


Figure 12: Infrared Red results at 250 °C (Left) and 350 °C (Right)

5. Discussion

5.1 Non-Arrhenius Decrystallization Behavior

The research team performed a kinetic study on the decrystallization of ZSM-5 in HLW in order to have a thorough understanding of the decrystallization behavior. The decrystallization rate was assumed to follow a pseudo-first order rate law as shown in the differential rate law equation below:

$$\frac{d[C]}{dt} = -k_{app}[C]$$

[C]: Crystallinity of Zeolite
 k_{app} : apparent rate constant

To verify the assumed rate law, the natural logarithm of the relative crystallinity at each temperature was plotted versus time, as shown in Figure 13a&b:

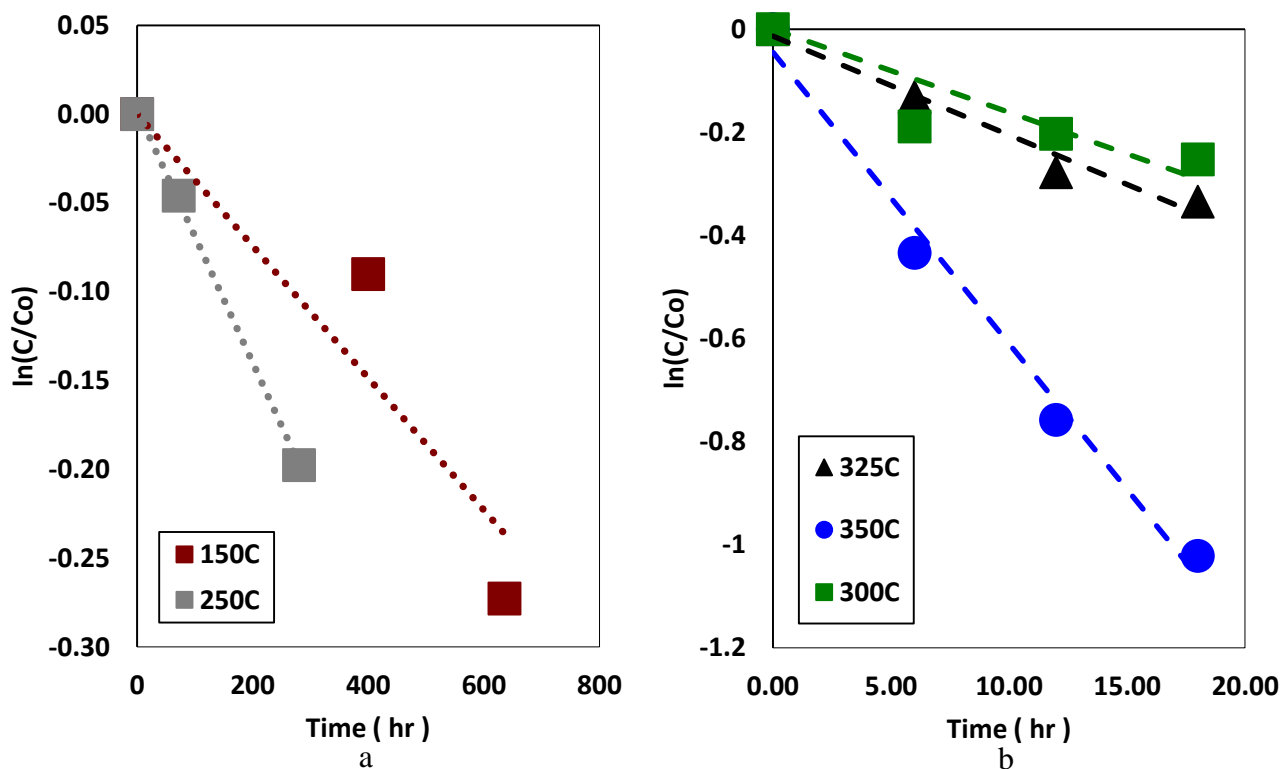


Figure 13: Natural logarithm of relative crystallinity as function of time

As the graphs show, the linear fit of the data implies that the decrystallization rate of ZSM-5 in HLW obeys a pseudo-first order rate law. The lower temperature plots in Figure 15a do not include data

taken after apparent zeolite stability at 75% relative crystallinity. Also, the initial increase in relative crystallinity was taken as time zero.

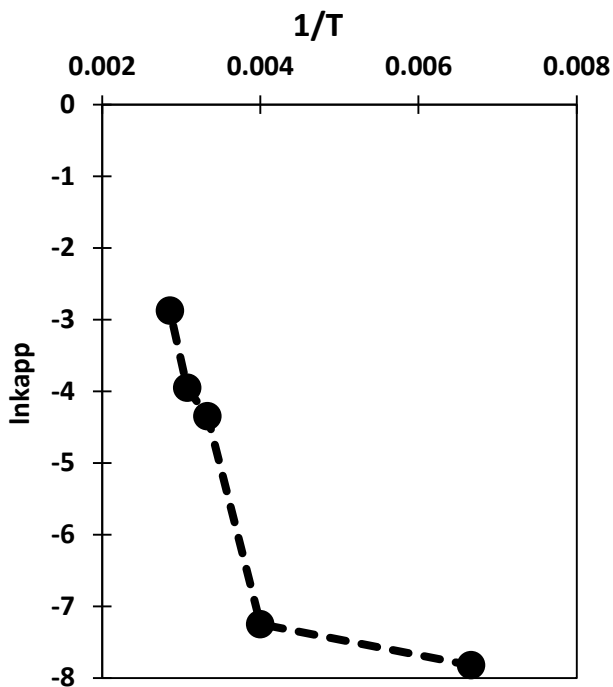


Figure 14: Natural logarithm of the apparent rate constant versus $1/T$

The apparent rate constant in the pseudo-first order rate law was investigated to determine the behavior of decrystallization; Arrhenius or non-Arrhenius. Figure 14 shows that the decrystallization behavior of ZSM-5 in HLW has non-Arrhenius behavior. The scientific literature attributes the non-Arrhenius behavior in aqueous medium to either; the change in ion concentration with temperature or the presence of multiple mechanisms.²² The research team investigated the two possibilities.

The change in ion concentration comes from the fact that the apparent rate constant of the decrystallization is composed of the real rate constant and the ion concentration as shown in the equation below.

$$k_{\text{app}} = k[\text{H}^+]$$

k: real rate constant
[H⁺]: concentration of ions

According to the possibility that the ion concentration changes with temperature, if the apparent rate constant is normalized by the concentration of ions in the solution as shown in the equation below, the real rate constant will show an Arrhenius behavior.

$$k = \frac{k_{\text{app}}}{[\text{H}^+]}$$

Therefore, the amount of ions in the solution had to be taken into account. In our system, there were two different sources of ions; the auto-ionization of water and the dissociation of the zeolite Brønsted acid sites in the solution. The ionic content of water has been investigated in previous studies showing that the temperature change impacts the water auto-ionization. Previous studies indicated that the ionic constant is a function of temperature. Ion product increases with temperature until it reaches temperatures around 300 °C where it decreases.^{34,35} On the other hand, the dielectric constant indicates the solvent's ability solvate ions decreases with increasing temperature in the subcritical region. Another source of ions in the solution is taken into consideration which originates from the disassociation of the acid sites in the zeolite. These factors are expected to impact the mechanisms of the reactions during the treatment of ZSM-5 in HLW. It is known that ZSM-5 is acidic, therefore, the team investigated the pH level of the solutions before and after the treatment. The untreated solutions of ZSM-5 (Si/Al=38 as 1 g) with DI water (40 mL) were found to be acidic at pH of 2.64. The treated samples showed an increase in the pH value in comparison to the untreated solution. The pH of the treated sample was not measured at the reaction condition, instead, it was measured after cooling the solution to room condition. This was done due to the lack of instrumentation that can measure the pH at the harsh reaction condition. Figure 15 shows that the values of pH followed a similar trend at the different temperatures. We do not fully understand the pH data. The loss of BAS and the formation of the insoluble EFAl might cause the increase in pH value between 0 hour (heating and cooling effect) and 6 hours.

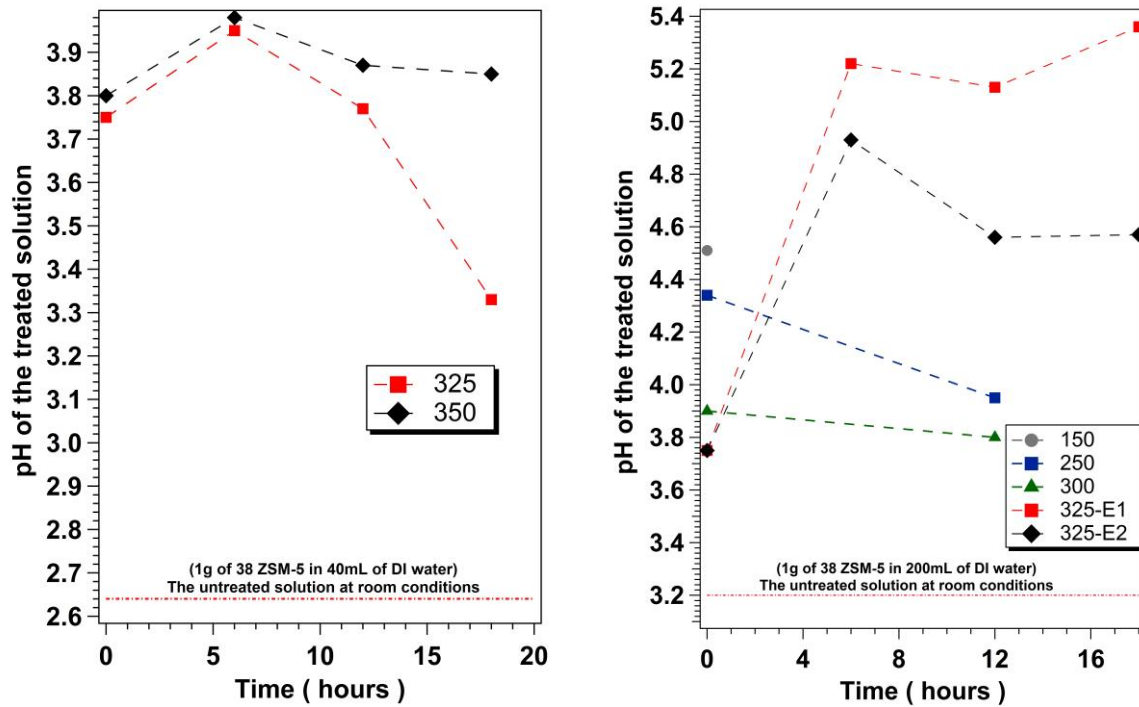


Figure 15: Measured pH level results

Therefore, the addition of these two sources would result in the amount of ions in the solution as shown in the equation below:

$$[H^+] = \frac{\sqrt{K_w(T, P)}}{\gamma_{\pm}(T, P)} + [H^+_{zeolite}](T)$$

K_w : the dissociation constant of water
 γ_{\pm} : the mean ion activity coefficient

The amount of ions from the dissociation of water was obtained using the reported value in the literature.²³ Also, the value of the mean ion activity coefficient was reported in the literature using an extended Debye–Hückel model.²² At the temperatures and pressures of our experiment, the mean ion activity coefficient was around one. The difficulty arose in finding the amount of ions from the dissociation of the zeolite Brønsted acid sites. The design team used the pH values that were obtained after the heating and cooling effect experiments, which were different from the pH of the untreated sample.

Now, the apparent rate constant was normalized based on the amount of ions in the solution and the graph was plotted again as shown in Figure 16 below.

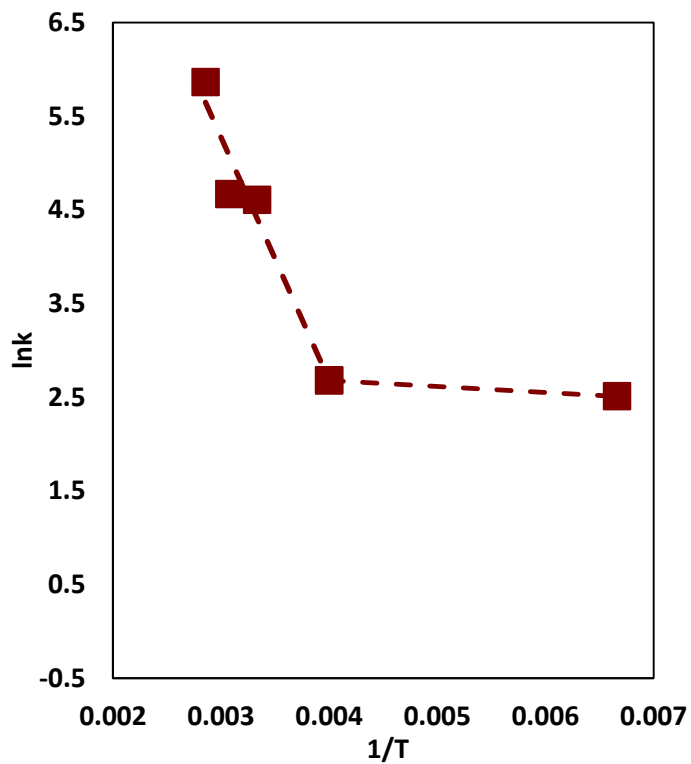


Figure 16: Natural logarithm of the real rate constant versus 1/T

The graph still shows a non-Arrhenius behavior. The research team believes that the inaccurate measurement of pH of the solution contributed to the behavior seen in Figure 16. Since there was no available method to measure the accurate pH of the solution, the team investigated the possibility of multiple decrystallization mechanisms by using IR and gas sorption data.

5.3 Decrystallization Mechanism

The two possible decrystallization mechanism of ZSM-5 in HLW, Dealumination and Desilication, are shown in Figure 18. Dealumination is the removal of Al from the framework to form EFAl, Desilication is the removal of Si from the framework.²

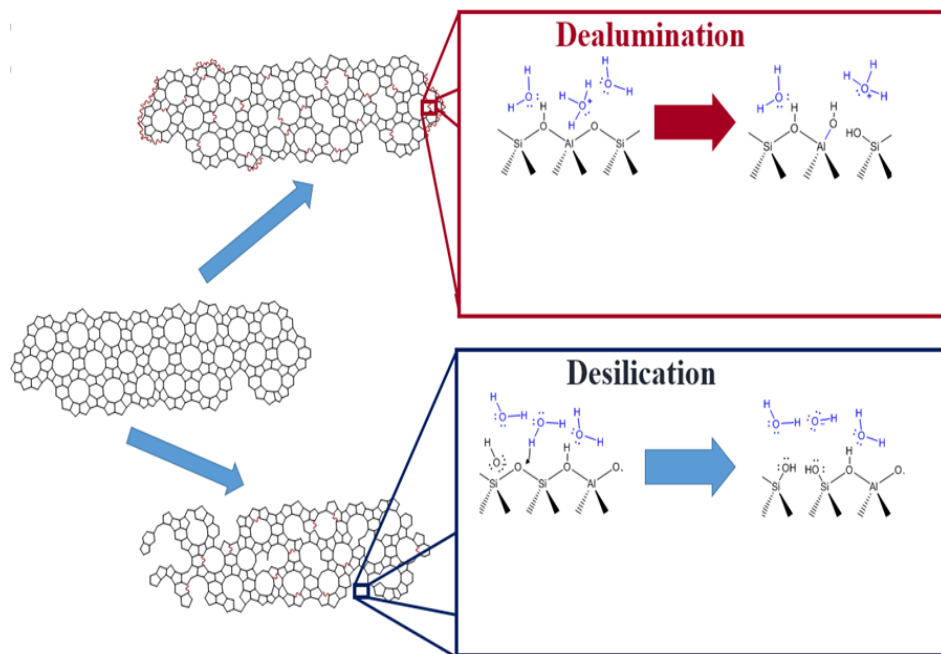


Figure 17: showing decrystallization mechanisms

To further investigate the decrystallization mechanism of ZSM-5 in HLW, the team compared results presented in You et al (Figure 17), on the effects of Dealumination and Desilication of H-ZSM-5.²⁴ From their results the main difference in the two decrystallization mechanism is the adsorption and desorption isotherm pathways. The adsorption and desorption isotherms for Dealumination have similar pathways, while the adsorption and desorption isotherms for Desilication have differing pathways. This difference in pathways is referred to as a hysteresis loop, and is associated with the filling and emptying of mesopores. Mesopores are created when Si is removed from high-silica zeolite framework of ZSM-5.³²

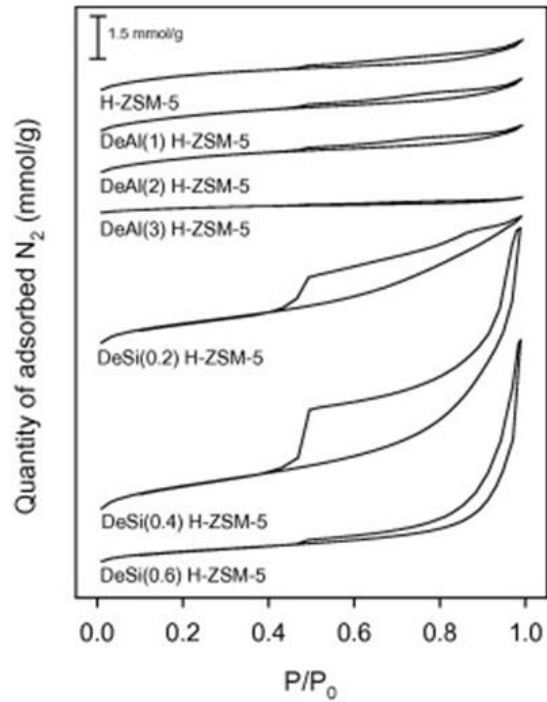


Figure 18: showing isotherms of dealuminated and desilicated H-ZSM-5.³²

In comparing the data presented in Figure 10 and Figure 18, we see that hysteresis loops are not present, thus indicating that the decrystallization mechanism of ZSM-5 in HLW is dealumination. Since dealumination is consistent at all temperatures, this eliminates the possibility of having non-Arrhenius behavior due to the presence of multiple mechanisms.

6. Conclusion

The stability of zeolites in hot liquid water is dependent on various factors. In analyzing the stability of zeolite ZSM-5 (Si/Al=38) in hot liquid water at temperatures ranging from 150-250 C and treatment time from 6 hr to 1000 hr, our team determined that decrystallization of ZSM-5 is due to a combination of thermal and ionic effects. The decrystallization of ZSM-5 in HLW is a result of the auto-ionization of water and the dissociation zeolite acid sites with increasing temperatures. Treating the zeolite in HLW at varying temperatures showed that the decrystallization rate of ZSM-5 is temperature dependent. Tracking the crystallinity over time showed that the decrystallization obeys a pseudo-first order rate. Temperature analysis of the pseudo first order rate constant indicates that the decrystallization of ZSM-5 follows a Non-Arrhenius behavior. The reason for the Non-Arrhenius behavior is due to change in water's ion concentration with temperature. Analyzing the samples with IR provided information to establish the fact that decrystallization of the zeolite show generation of EFAL and loss of Brønsted acid sites and silanol groups. The main decrystallization mechanism is dealumination. In this report, the mechanism of decrystallization in HLW is an important finding that could further allow the explanation of other aspects of the substance such as the pH of the solution. The treatment conditions examined in this study are representative of some of the new feedstock and chemical technologies, such as oil upgrading and biofuel production, that take place in the aqueous phase. The results presented provide guidance for use of zeolites in these industrially relevant reactions and show that the stability of ZSM-5 in high temperature aqueous environments needs to be examined carefully.

7. Recommendations

In our research we reached few times a point where more questions were created than solved. This might be attributed to the lack of understanding of the ZSM-5 behavior in HLW by the scientific community. For this reason, a more thorough analysis of data should be done so that the full scale of its characteristics can be analyzed. For this exact reason more temperatures should be investigated and especially for temperatures of 175 to 275°C where there is a sudden transition of the rate of decrystallization observed. The results retrieved would be more trustworthy if the data are reproduced in a manner to double check for inconsistency and decrease of random error created when running the experiment. The crystallinity after heating and cooling effect needs to be examined in more detail. During the end of our research a pH study was initiated but was proved to be more complicated than expected, showing that the time needed for the establishment of such a study was not sufficient. A study explaining the inconclusive trend of the acidity of the solution during treatment should be conducted at the reaction condition and justified. Other analytical tools such as Si- and Al-NMR, ICP, XPS. Si- and Al-NMR could provide further information to understand the mechanism. ICP-MS (Inductively Coupled Plasma Mass Spectrometry) can help identify and quantify elemental constituents in the zeolite solution. XPS (X-ray Photoelectron Spectroscopy) can be used to analyze the surface chemistry of the zeolite before and after treatment.

Recommended Computational Work

To gain a better understanding of the ZSM-5 degradation mechanism in HLW at the molecular level, our research team recommends performing a computational study. There are multiple ways to utilize computational tools. These include, but are not limited to, studying the thermodynamic and kinetics properties of the possible degradation mechanisms for ZSM-5. According to the scientific literature, the most common method to perform computational studies of ZSM-5 is Density Functional Theory (DFT). Based on Hohenberg and Kohn (HK) theorems, DFT provides a strong basis for the development of computational strategies for obtaining information about the energetics, structure and properties of atoms and molecules.²⁵ HK theorem states that the electron density $\rho(r)$, determines the internal potential, $v(r)$. $\rho(r)$ determines the total number of electrons, N and is represented by the equation:

$$N = \int \rho(r) dr$$

N determines the molecular Hamiltonian, H_{op} , which is linked to the energy of the system, E , by the Schroödinger's equation:

$$H_{op}\Psi = E\Psi$$

Where Ψ , is the electronic wave function. Consequently, E is a function of ρ :

$$E = E_v[\rho]$$

ZSM-5 has a large unit cell (288 atoms 96 silicon atoms and 192 oxygen atoms), which may lead to long computational time, and thus it may be important to focus on only one region of the zeolite.²⁶ Jungsuttiwong et al focused on isomorphously substituted ZSM-5 zeolites and used an embedded cluster method to model the most important regions of the chemistry of the system as that surrounding the active site and the adsorbate, and treated these regions explicitly within full quantum mechanical formalism as an isolated system and adding the effects of the remaining crystal framework in the Hamiltonian of the quantum region.

The first step in performing DFT simulations is to construct a model of the ZSM-5. Three examples of models are 5T, 12T and E-ONIOM. Jungsuttiwong et al used the embedded approach, E-ONIOM model with the B3LYP/6-31G (d,p) level of theory for their study to study the structure of BAS and get energetic information. As seen in Figure 19 the 5T model has a total of 22 atoms with a formal of

$\text{Si}_4\text{AlO}_4\text{H}_{13}$. It is part of a 10-membered ring of the ZSM-5 zeolite, consisting of five tetrahedrally coordinated atoms (Si, Al).

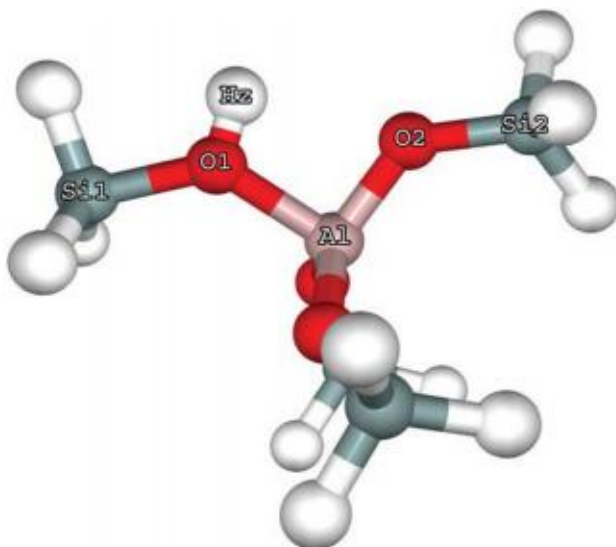


Figure 19: The 5T model.²⁶

As seen in Figure 20, the 12T model has a total of 49 atoms with a formula of $\text{Si}_{11}\text{AlO}_{12}\text{H}_{25}$. Also, the active site was chosen to be the T12 site because it was found to be among the most stable sites for Al substitution.²⁷

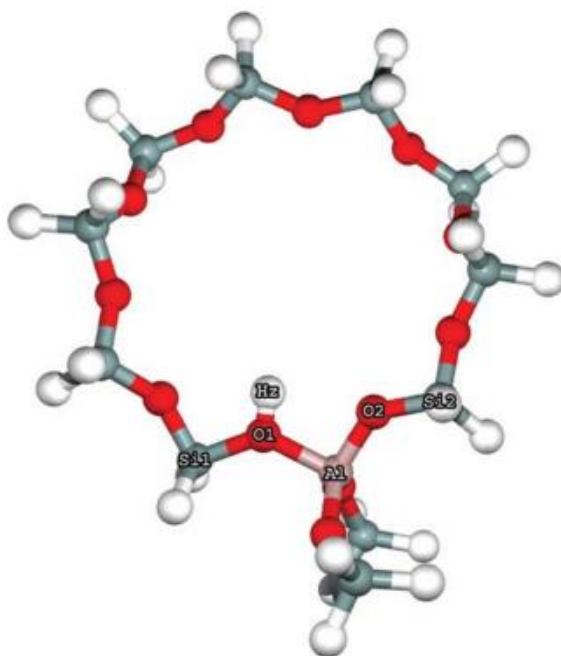


Figure 20: The 12T model.²⁶

The E-ONIOM model as seen in Figure 21, is used to include the long-range interactions of the zeolite lattice beyond 12T, Figure 20.^{27a} In these three models, H-atoms are used to cap the dangling atoms. These hydrogen atoms are located along the direction of corresponding Si-O bonds. The T12 site was chosen to be the active sites as it was found to be the most stable site for Al substitution.²⁷

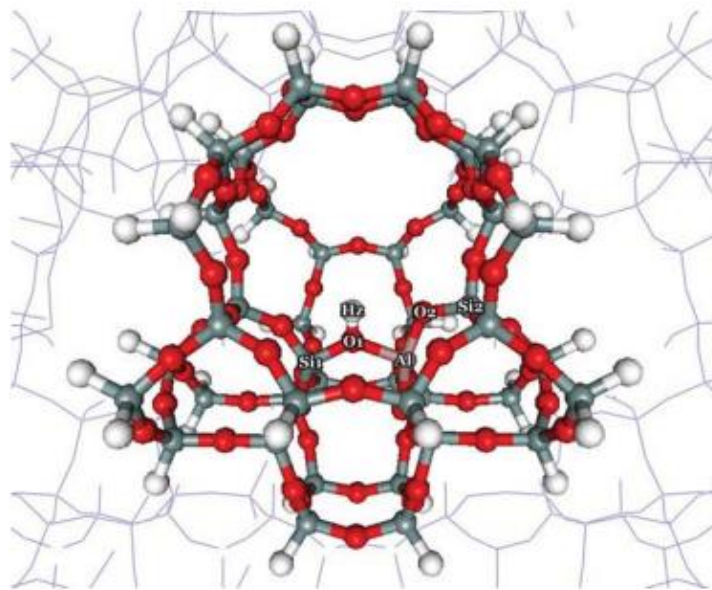


Figure 21: The Embedded ONIOM model.²⁶

Our team suggests that performing DFT studies using each of these models for the reactants and products associated with dealumination and desilication degradation mechanisms. When optimizing the geometry of the structures for each computational run the following procedure is recommended: (1) Fix the position Si-H atoms and (2) Set the bond length of Si-H to 1.43Å.²⁸ A thermodynamic study must be conducted to determine the heat of reaction for both desilication and dealumination from calculated energies. The most exothermic reaction should be identified as the most stable product. Additionally, protons and hydroxide ions should be used instead of water. The hydrogen bonds between the molecules should also be considered.

Malola et al performed kinetic studies by examining detailed reaction paths for zeolite dealumination and desilication using DFT.²⁸ In their study, they found that several systematic differences favor dealumination over desilication under steaming conditions. Also, the difference between Si and Al may be explained by the well-known coordination flexibility of the Al and the higher polarity of the

Al-induced Bronsted site. Moreover, the study recommended that further work investigate the effects of allowing water clusters instead of single water molecules to reside within the zeolite pores during dealumination and desilication.

8. References

1. (a) Zhang, L.; Chen, K.; Chen, B.; White, J. L.; Resasco, D. E., Factors that Determine Zeolite Stability in Hot Liquid Water. *Journal of the American Chemical Society* **2015**, *137* (36), 11810-11819; (b) Müller, U.; Reichert, H.; Robens, E.; Unger, K.; Grillet, Y.; Rouquerol, F.; Rouquerol, J.; Pan, D.; Mersmann, A., High-resolution sorption studies of argon and nitrogen on large crystals of microporous zeolite ZSM-5. *Fresenius' Zeitschrift für analytische Chemie* **1989**, *333* (4-5), 433-436; (c) Hartman, R. L.; Fogler, H. S., Understanding the dissolution of zeolites. *Langmuir : the ACS journal of surfaces and colloids* **2007**, *23* (10), 5477-84.
2. Ravenelle, R. M.; Schüßler, F.; D'Amico, A.; Danilina, N.; van Bokhoven, J. A.; Lercher, J. A.; Jones, C. W.; Sievers, C., Stability of Zeolites in Hot Liquid Water. *The Journal of Physical Chemistry C* **2010**, *114* (46), 19582-19595.
3. Bhatia, S., *Zeolite catalysts: principles and applications*. CRC press: 1989.
4. (a) Beyerlein, R. A.; Choi-Feng, C.; Hall, J. B.; Huggins, B. J.; Ray, G. J., Effect of Steaming on the Defect Structure and Acid Catalysis of Protonated Zeolites. *Top Catal* **1997** SRC - *GoogleScholar*, 27-42; (b) Triantafillidis, C. S.; Vlessidis, A. G.; Evmiridis, N. P.; Dealuminated, H.; Y., Influence of the Degree and the Type of Dealumination Method on the Structural and Acidic Characteristics of H- Ind. *Eng Chem Res* **39** 2000 SRC - *GoogleScholar*, 307-319; (c) van Donk, S.; Janssen, A. H.; Bitter, J. H.; de Jong, K. P., Characterization, and Impact of Mesopores in Zeolite Catalysts. *Catal. Rev.-Sci. Eng* (2003), 297-319.
5. (a) Sanz, J.; Fornes, V.; Corma, A., Extraframework Aluminum in Steam- and SiCl₄-dealuminated Y Zeolite. *J. Chem. Soc., Faraday Trans* (1988 SRC - *GoogleScholar*), 3113-3119; (b) Stockenhuber, M.; Lercher, J. A., Characterization and removal of extra lattice species in faujasites. *Microporous Materials* **1995**, *3* (4-5), 457-465.
6. Breck, D. W.; Flanigan, E. M., Synthesis and properties of union carbide zeolites L, X and Y," in *Molecular Sieves. ociety of Chemical Industry, London, UK* **1968**, (1968 SRC - *GoogleScholar*), 47-60.
7. Carvajal, R.; Chu, P.-J.; Lunsford, J. H., The role of polyvalent cations in developing strong acidity: A study of lanthanum-exchanged zeolites. *Journal of Catalysis* **1990**, *125* (1), 123-131.
8. mith, R. L.; Jin, F.; Zhou, Q.; Wu, B., Water Under Hydrothermal, Supercritical, and High Pressure Conditions as Key to Developing Green Processes and New Technologies.
9. (a) Mokaya, R., Al Content Dependent Hydrothermal Stability of Directly Synthesized Aluminosilicate MCM-41. *The Journal of Physical Chemistry B* **2000**, *104* (34), 8279-8286; (b)

Shen, S. C.; Kawi, S., Understanding of the Effect of Al Substitution on the Hydrothermal Stability of MCM-41. *The Journal of Physical Chemistry B* **1999**, *103* (42), 8870-8876.

10. Baerlocher, C.; McCusker, L. B.; Olson, D. H., *Atlas of zeolite framework types*. Elsevier: 2007.

11. ZEOMICS - View Structure. http://helios.princeton.edu/zeomics/cgi-bin/view_structure.pl?src=iza (accessed Apr 22, 2016).

12. Lei, X.-g.; Jockusch, S.; Ottaviani, M. F.; Turro, N. J., In situ EPR investigation of the addition of persistent benzyl radicals to acrylates on ZSM-5 zeolites . Direct spectroscopic detection of the initial steps in a supramolecular photopolymerization. **2003**.

13. Brunner, G., *Hydrothermal and supercritical water processes*. Elsevier: 2014; Vol. 5.

14. Vácha, R.; Buch, V.; Milet, A.; Devlin, J.; Jungwirth, P., Autoionization at the surface of neat water: is the top layer pH neutral, basic, or acidic? *Physical Chemistry Chemical Physics* **2007**, *9* (34), 4736-4747.

15. Peterson, A. A.; Vogel, F.; Lachance, R. P.; Fröling, M.; Antal Jr, M. J.; Tester, J. W., Thermochemical biofuel production in hydrothermal media: a review of sub-and supercritical water technologies. *Energy & Environmental Science* **2008**, *1* (1), 32-65.

16. Begley, J. A.; Landes, J. D., American Society for Testing and Materials. *ASTM STP* **1972**, *D5758*.

17. Sing, K., The use of nitrogen adsorption for the characterisation of porous materials. *Colloids and Surfaces A: Physicochemical and Engineering Aspects* **2001**, *187-188*, 3-9.

18. Damjanovic, L.; Auroux, A.; Chester, A. W.; Derouane, E. G., *Zeolite Characterization and Catalysis: A Tutorial*. Springer. Londres (Inglaterra): 2010.

19. Nicolet, T., Introduction to fourier transform infrared spectrometry. *Information booklet* **2001**.

20. Ennaert, T.; Geboers, J.; Gobechiya, E.; Courtin, C. M.; Kurttepel, M.; Houthoofd, K.; Kirschhock, C. E. A.; Magusin, P. C. M. M.; Bals, S.; Jacobs, P. A.; Sels, B. F., Conceptual Frame Rationalizing the Self-Stabilization of H-USY Zeolites in Hot Liquid Water. *ACS Catalysis* **2015**, *5* (2), 754-768.

21. (a) Methanol to hydrocarbons: spectroscopic studies and the significance of extra-framework aluminium. **1999**, *29* (Issues 1–2), 91–108; (b) Groen, J. C.; DelftChemTech, D. U. o. T., Julianalaan 136, 2628 BL Delft, The Netherlands, Fax: (+31) 15-278-4452; Peffer, L. A. A.; DelftChemTech, D. U. o. T., Julianalaan 136, 2628 BL Delft, The Netherlands, Fax: (+31) 15-278-4452; Moulijn, J. A.; DelftChemTech, D. U. o. T., Julianalaan 136, 2628 BL Delft, The Netherlands, Fax: (+31) 15-278-

- 4452; Pérez-Ramírez, J.; Catalan Institution for Research and Advanced Studies (ICREA) and Institute of Chemical Research of Catalonia (ICIQ), A. P. C. s. n., 43 007 Tarragona, Spain, Mechanism of Hierarchical Porosity Development in MFI Zeolites by Desilication: The Role of Aluminium as a Pore-Directing Agent. *Chemistry – A European Journal* **2016**, *11* (17), 4983-4994.
22. Taylor, J. D.; Pacheco, F. A.; Steinfeld, J. I.; Tester, J. W., Multiscale Reaction Pathway Analysis of Methyl tert-Butyl Ether Hydrolysis under Hydrothermal Conditions. *Industrial & Engineering Chemistry Research* **2002**, *41* (1), 1-8.
23. Bandura, A. V.; Data, J., The Ionization Constant Of Water over Wide Ranges of Temperature and Density. *Journal of Physical and Chemical Reference Phys Chem Ref Data* *35 15 2006 SRC - GoogleScholar*.
24. You, S. J.; Park, E. D., Effects of dealumination and desilication of H-ZSM-5 on xylose dehydration. **2014**, *186* (2014), 121-129.
25. Geerlings, P.; De Proft, F.; Langenaeker, W., Conceptual density functional theory. *Chemical reviews* **2003**, *103* (5), 1793-873.
26. Jungsuttiwong, S.; Lomratsiri, J.; Limtrakul, J.; Substituted, Z. S. M.; Embedded, D. F. T.; F., U. F., Characterization Of Acidity in [B], [Al], and [Ga] Isomorphously Int. *J Quantum Chem International Journal of Quantum Chemistry* *111* **2011**, *5 SRC - GoogleScholar*, 2275-2282.
27. (a) Injan, N.; Pannorad, N.; Probst, M.; Limtrakul, J., Pyridine adsorbed on H-Faujasite zeolite: Electrostatic effect of the infinite crystal lattice calculated from a point charge representation. *International Journal of Quantum Chemistry* **2005**, *105* (6), 898-905; (b) Derenzo, S. E.; Klintonberg, M. K.; Weber, M. J., Determining point charge arrays that produce accurate ionic crystal fields for atomic cluster calculations. *The Journal of Chemical Physics* **2000**, *112* (5), 2074-2081.
28. Zygmunt, S. A.; Curtiss, L. A.; Iton, L. E.; Erhardt, M. K.; Zeolite, H.; Chemistry, J., Computational Studies Of Water Adsorption in the ZSM-5. *The Journal of Physical Phys Chem* *100 1996 SRC - GoogleScholar*, 6663-6671.

Appendix

Tables of relative crystallinity results

% Crystallinity	
Average cooling time= 5 minutes	
Average heating time= 15 minutes	
P=2700 psi	
Uncertainty= +/- 4%	
T= 150 C	
Time (hr)	% Crystallinity
0	100%
187	101.43%
400	91.39%
635	76.13%
1000	76.41%

% Crystallinity			
Average cooling time= 10 minutes			
Average heating time= 25 minutes			
P=3600 psi			
Uncertainty= +/- 3.3%			
Run A: T=250 C			
Time (hr)	RunA1	RunA2	RunA3
0	100%	100%	100%
6	101.62%	102.35%	106.55%
12	107.68%	108.09%	99.59%
24	99.46%	97.99%	105.17%
48	95.87%	95.68%	92.96%
72	92.67%	94.01%	99.84%
280	82.07%		
492	81.45%		

% Crystallinity	
Average cooling time= 10 minutes	
Average heating time= 35 minutes	
Uncertainty= +/- 4%	
Run C3: T=300 C	
P (psi)	3600
Time (hr)	%Crystallinity
0	100%
6	82.78%
12	81.61%
18	77.66%

% Crystallinity	
Average cooling time= 10 minutes	
Average heating time= 35 minutes	
Uncertainty= +/- 4%	
Run E3: T=325 C	
P (psi)	2700
Time (hr)	%Crystallinity
0	100%
6	87.64%
12	75.77%
18	71.55%

% Crystallinity	
Average cooling time= 10 minutes	
Average heating time= 40 minutes	
Uncertainty= +/- 4%	
Run B3: T=350 C	
P (psi)	3600
Time (hr)	%Crystallinity
0	100%
6	64.80%
12	46.88%
18	35.98%

MQP Poster



Non-Arrhenius Dealumination of ZSM-5 in Hot Liquid Water

Ibrahim Abu Muti (CHE), Abdullah Almaymuni (CHE), Nyoca Davis (CHE), Iordanis Kesisoglou (CHE)
 Advisor: Professor M. Timko (CHE) Co-Advisor: A. Deskins (CHE)



Motivation

Many industrial processes require strong acid catalysts. Recent studies have shown that ZSM-5 zeolite has advantages over other acid catalysts in aqueous phase reactions. The scientific literature is limited in the fundamental understanding of the framework stability of ZSM-5 in hot liquid water (HLW). Previous degradation studies in HLW have shown limited stability for reactions at 200°C up to 6hrs, but many processes require higher temperature stability over longer times. Fundamental understanding of the degradation of ZSM-5 at high temperatures is lacking. Complicating matters, the properties of water changes dramatically at temperatures above 200°C, thus playing a potential role in the degradation rate.

Goal:

- Develop a fundamental understanding of the decrystallization mechanism of ZSM-5 in HLW.

Objectives:

- Measure the crystallinity of ZSM-5 after treatment in HLW.
- Analyze the rate of decrystallization of ZSM-5.
- Determine the mechanism of ZSM-5 decrystallization.

Non-Arrhenius Behavior: XRD

Intensity vs 2θ and Relative crystallinity vs Time (hours) plots showing the effect of temperature on decrystallization rate.

- XRD shows loss of crystallinity over time.
- Increasing the temperature increases the decrystallization rate.

Decrystallization Mechanism

Dealumination: Acid catalyzed, No mesopores
 Desilication: Base catalyzed, Mesopores

- Look for Alumina (IR-Drifts)
- Look for mesopores (Gas Sorption)

Methodology

Treatment: ZSM-5 in HLW at temperature (T) and pressure (P).

Preparation: ZSM-5

Analytical tools:

- SEM (surface morphology)
- XRD (crystallinity)
- IR (chemistry)
- Gas Sorption (mechanism)

Kinetic Analysis

$$\frac{d[C]}{dt} = -k_{app}[C]$$

$$[C]: \text{Crystallinity of Zeolite}$$

$$\hat{k}_{app} = k_1[H^+]$$

$$k = \frac{k_{app}}{[H^+]}$$

ZSM-5 decrystallization in HLW obeys a pseudo-first order rate law.

- Auto-ionization of water increases the H⁺ concentration.
- ZSM-5 strong acid sites dissociate in liquid water, adding to the H⁺ concentration.

$$[H^+] = \frac{K_w(P, P)}{\gamma \alpha (T, T)} = [H^+]_{200/273} (T, T)$$

ZSM-5 decrystallization in HLW follows a non-Arrhenius behavior due to the changes in H⁺ concentration with temperature.

IR-Drifts

Loss of Brønsted acid sites, Loss of silanol groups (SiOH), Generation of EFAI.

Gas Sorption

No Hysteresis = No internal desilication, Increase in temperature and time leads to decrease in pore volume = pore blocking.

Surface Morphology: SEM

HLW treatment resulted in the transformation of the ZSM-5 crystal to an amorphous phase that resembles a flower.

Conclusions

The decrystallization of ZSM-5 in HLW follows non-Arrhenius rate behavior due to the change in H⁺ concentration. This change is a result of the auto-ionization of water and the dissociation of zeolite acid sites with the change in temperature. Evidence suggests that decrystallization of ZSM-5 in HLW occurs primarily due to dealumination.

References

- Campbell et al. *J. Cat.* 1998
- Ravenelle et al. *J. Phys. Chem.* 2010
- American Society for Testing and Materials (D5753)
- You, Park. *Microporous and Mesoporous Materials.* 2014, 188, 121–128.
- Resasco et al. *J. Am. Chem. Soc.* 2015

Acknowledgement

Professor Timko, Professor Deskins, Professor Sisson, Professor Tompsett, and Thomas Parrington, Timko's Lab: Alex Maag, Avery Brown, Maksim Tyufekchiev, and Azadeh Zaker. WPI Chemical Engineering Department. Saudi Aramco provided partial funding for this work.

Figure 22: The MQP project poster